

**How to Cite:**

Hasson, S. S., & Alsammarraie, A. M. (2022). Synthesis of nickel oxide nanoparticles by Sol-gel method. *International Journal of Health Sciences*, 6(S7), 6915-6924.

<https://doi.org/10.53730/ijhs.v6nS7.13692>

# Synthesis of nickel oxide nanoparticles by Sol-gel method

**Sura Sabri Hasson**

Department of Chemistry/College of Science/university of Baghdad/Baghdad/Iraq

**Abdulkareem M.A. Alsammarraie**

Department of Chemistry/College of Science/university of Baghdad/Baghdad/Iraq

**Abstract**---Nickel oxide NPs are widely recognized as excellent photocatalysts due to their unique optical features such as bandgap energy, retention time, strong light absorption, electron-hole recombination duration, and significant negative oxidation potential of excited electrons. NiO nanoparticles were successfully created using a combination of nickel hexahydrate precursor, ethanol, and distilled water. Nickel hexahydrate NiO was employed as a nickel precursor to create nickel oxide nanoparticles (NO<sub>3</sub>).6H<sub>2</sub>O, distilled water, and stirring until solution homogeneity were used to make alkaline sodium hydroxide, and the alkaline solution was distilled into a homogenous solution on a magnetic stirrer at 75 °C. A thick green solution was produced at pH=12. The surface morphology and nanoparticle size of the as-prepared NiO nanoparticles were estimated using SEM and AFM images of spherical NiO particles with sizes of about 26.80 nm and 37.96 nm. The cubic crystal structure of NiO was disclosed using X-ray Diffraction (XRD). NiO NP absorption spectra in the UV and visible ranges show blue has a maximum wavelength of 341 nm. The nickel oxide band is seen at 627 in Fourier transform infrared (FTIR) spectroscopy.

**Keywords**---Nickel Oxide nanoparticle; hydrothermal method; UV-visible spectroscopy; X-ray diffraction (XRD); scanning electron microscopy (SEM).

## Introduction

This method is used to convert metal alkoxides or liquid precursors into solid nanomaterials by condensation and hydrolysis. A sol-gel process, as described in, entails the production of inorganic networks by sol formation (colloidal suspension) and sol gelation into gel, which is a continuous liquid phase network<sup>[1]</sup>. The most common precursors utilized to manufacture these colloids

are metals or metalloid components surrounded by reactive ligands. When the initial components come into contact with water or diluted acids, they are treated to form dispersible oxides and sol. This sol-gel transition governs the size and shape of the nanomaterials by separating the liquid from the sol. When calcined, the gel transforms into oxide<sup>[2]</sup>. The hydrolysis processes are used in the production of nanomaterials by the sol-gel method.

**Hydrolysis:  $\text{MOR} + \text{H}_2\text{O} \rightarrow \text{MOH} + \text{ROH}$**

**Condensation:  $\text{MOH} + \text{ROM} \rightarrow \text{M-O-M} + \text{ROH}$ .**

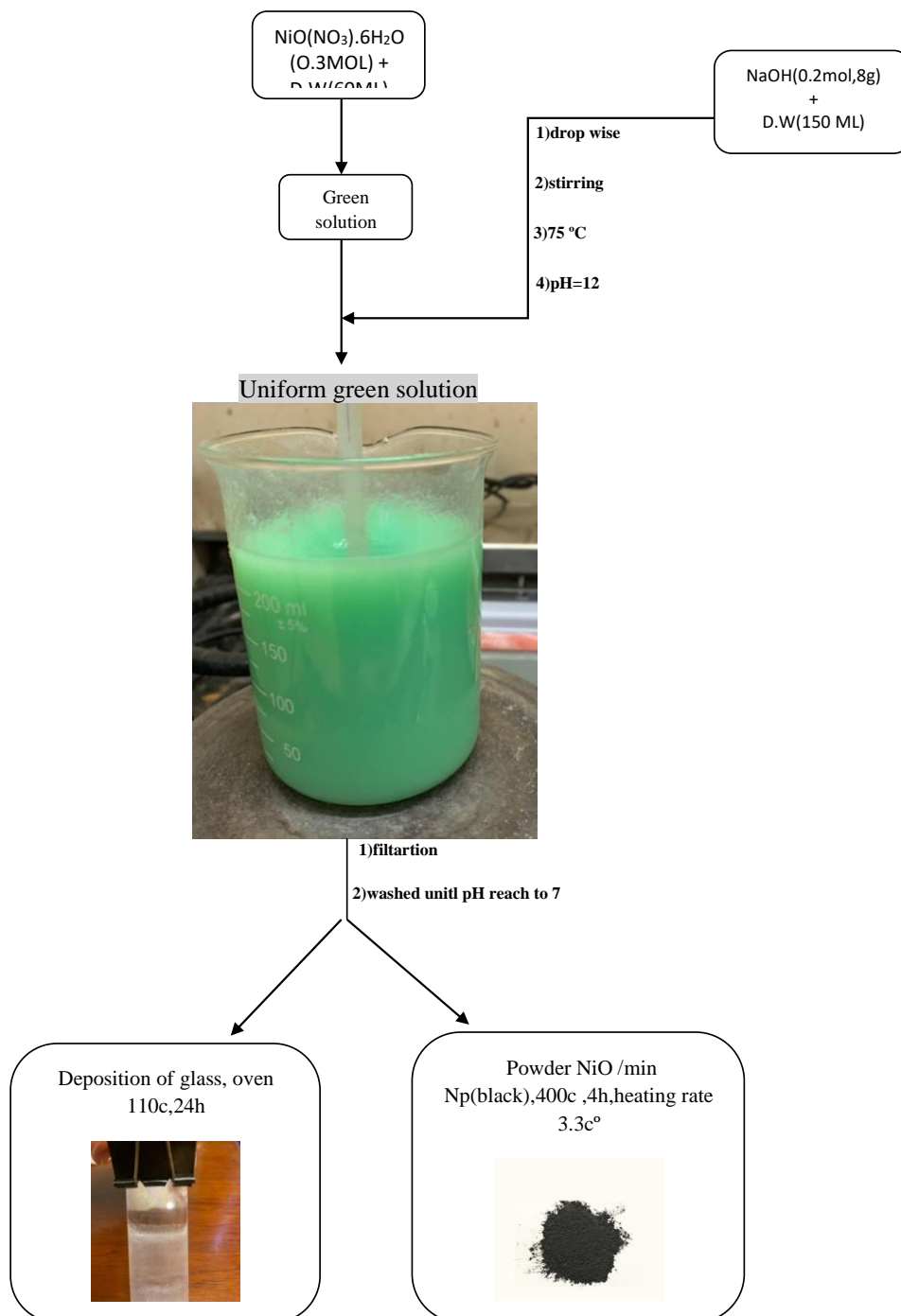
Nanoparticles can be prepared easily by sol-gel, whether they are films, fibers, ceramics, or glass. has a number of advantages over other methods such as inexpensive equipment, homogenous product and easily in processing <sup>[3, 4]</sup>. Sol-gel method will produce small particle size and uniform distribution particle with high homogenous, the size of the nanocomposites was distinct and altered in a fairly simple synthesis procedure, ranging between 2 and 4<sup>[5]</sup>. The investigation of atomic absorption revealed that the peak varied between 300 and 340 nanometers as particle size increased; also, it is regarded as a successful approach for processes involving transitions. It is ionic and necessitates an underlying temperature as well as a sufficient reaction for all of the chemicals involved in the reaction<sup>[6]</sup>.

NiO is a semiconductor which has a kind of important inorganic material, is stoichiometric and antiferromagnetic. It has a wide, stable and stable bandgap of 3.6 to 4.0 eV in material, and is a natural p-type semiconductor with high electron transfer performance<sup>[7, 8]</sup>, and its type of conductivity is related to intrinsic oxygen opportunities<sup>[9]</sup>. The structural property of particles (particle size, distribution, morphology) is closely related to the preparation technology. Few methods for preparing NiO have been reported<sup>[10] [11]</sup>.

## **2. Experimental Part**

Preparation of nanoparticles by sol-gel using nickel hexahydrate  $\text{NiO}(\text{NO}_3) \cdot 6\text{H}_2\text{O}$ , distilled water, 0.03 (8.72 g) mol of  $\text{NiO}(\text{NO}_3) \cdot 6\text{H}_2\text{O}$  dissolved in 60 mL of deionized water (DW) with good stirring until the solution became a homogeneous green color (sample A), then to prepare a medium alkaline as well. 0.2 mol (8 g) of NaOH was dissolved in 150 mL of DW (sample B). Then, (B) was added dropwise by burette to a (A) on a magnetic stirrer at 75°C and 300 rpm until a uniform green solution was obtained. Then, the pH of the solution was measured as 12. Then it was passed through the filter and a gelatinous solution was obtained and to obtain a uniform powder the samples were placed in an oven for 4 hours at a heating rate of 3.3 °C per minute at 400 °C for production . Black nanoparticles.

Sol–Gel method include the following schematic diagram :-



### 3.Result and discussion

#### 3.1XRD analysis

XRD pattern shows peaks at  $2\theta$  of  $43.3^\circ$ ,  $44.7^\circ$ ,  $62.9^\circ$ , shown figure (3.1.1) which relate to the reflection planes (111), (200) and (220) respectively, All these peaks are crystalline characteristics of formation of phase pure nickel oxide with cubic structure according to standard card (JCPDS No. 047-104900) (Nalage et al., 2012). Size of the formed crystallites can be calculated by Debye–Scherrer equation<sup>[12]</sup>:

$$D = k\lambda / \beta \cos\theta$$

The main particles size of the NiO nanocomposite approximately

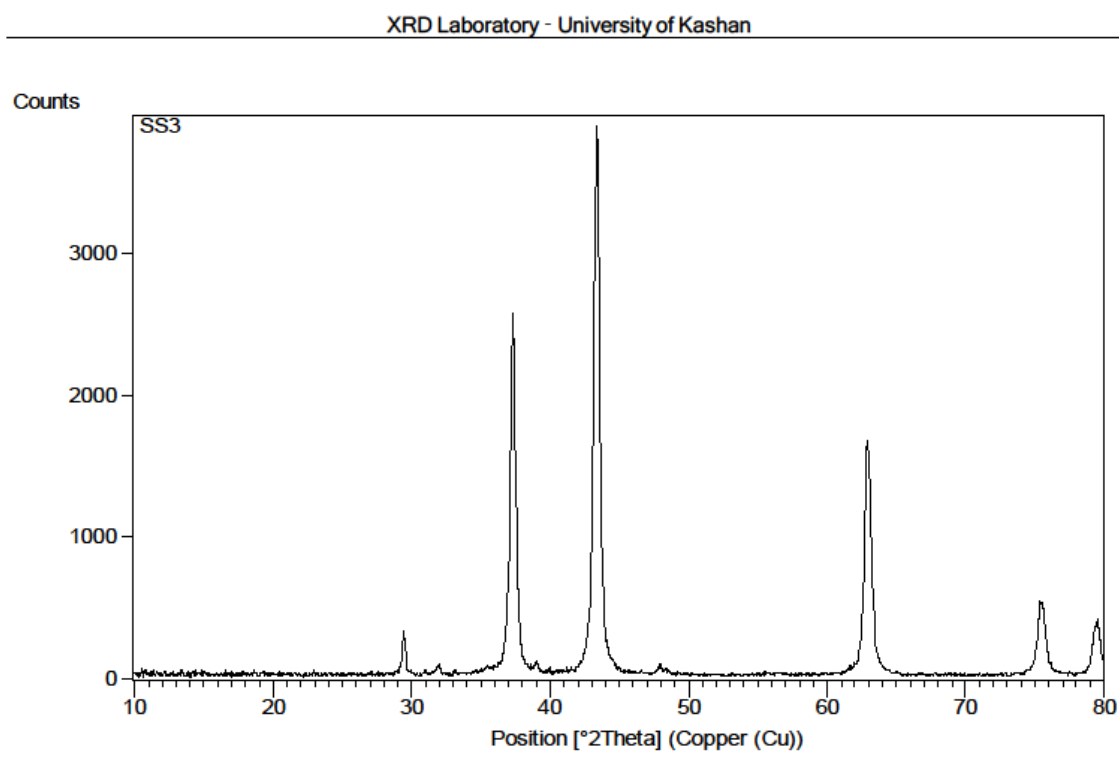
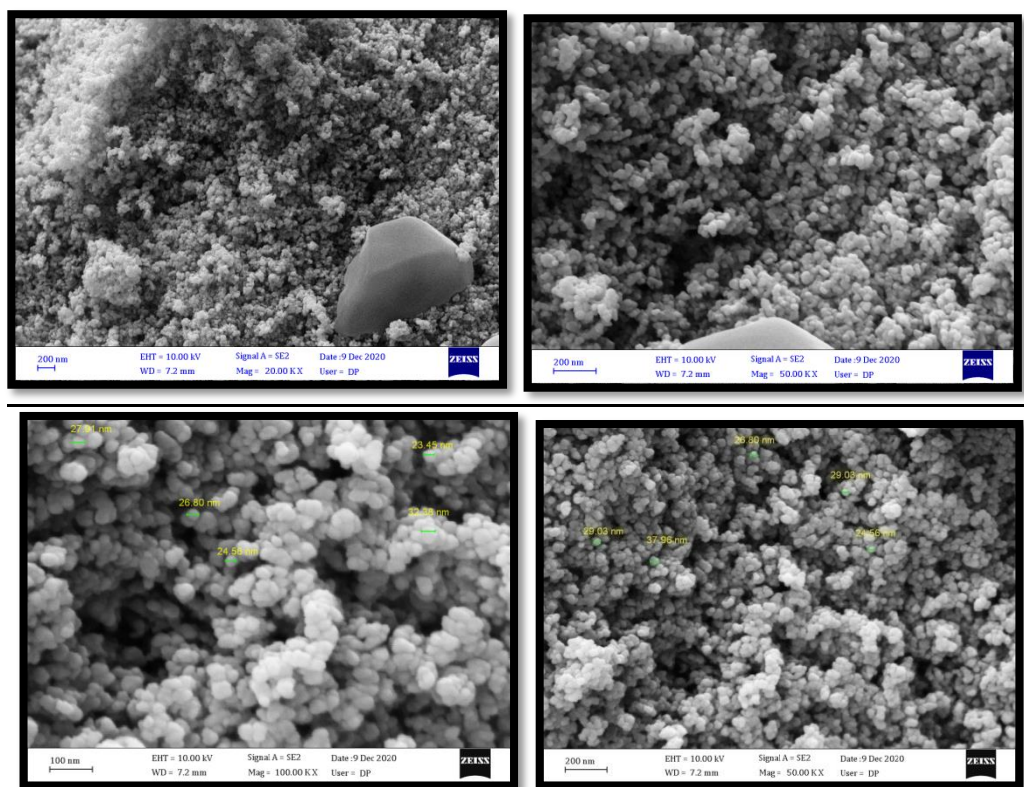


**Figure (1) : XRD Pattern of NiO nanostructure by sol-gel method.**

#### 3.2.SEM images

Nanoparticle diagnostics showed different shapes and sizes of nanocomposites, and this has been demonstrated by SEM. SEM images were recorded of nickel oxide nanoparticles of different shapes and sizes and indicated that the sol-gel

compounds contain small spherical nanoparticles. The SEM image of the NiO showed that the sample powder contained types of spherical nanoparticles and the particle size ranged between (26.80nm\_37.96nm). As shown in the figure (2).

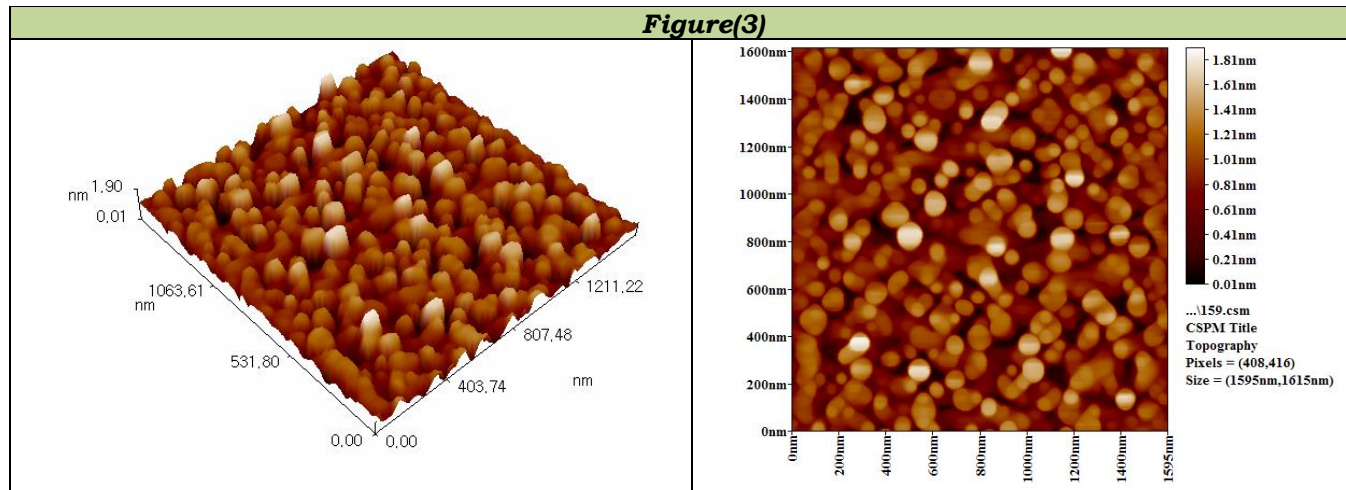


**figure (2) show powder nanoparticles of NiO by sol-gel**

### **3. 3. Atomic Force Microscopy (AFM)**

The AFM image of NiO nanoparticles in two and three dimensions are shown in figures(3) respectively. The results of AFM for NiO nanoparticles showed that the diameter of the particles were average of 50nm and 63nm receptively.

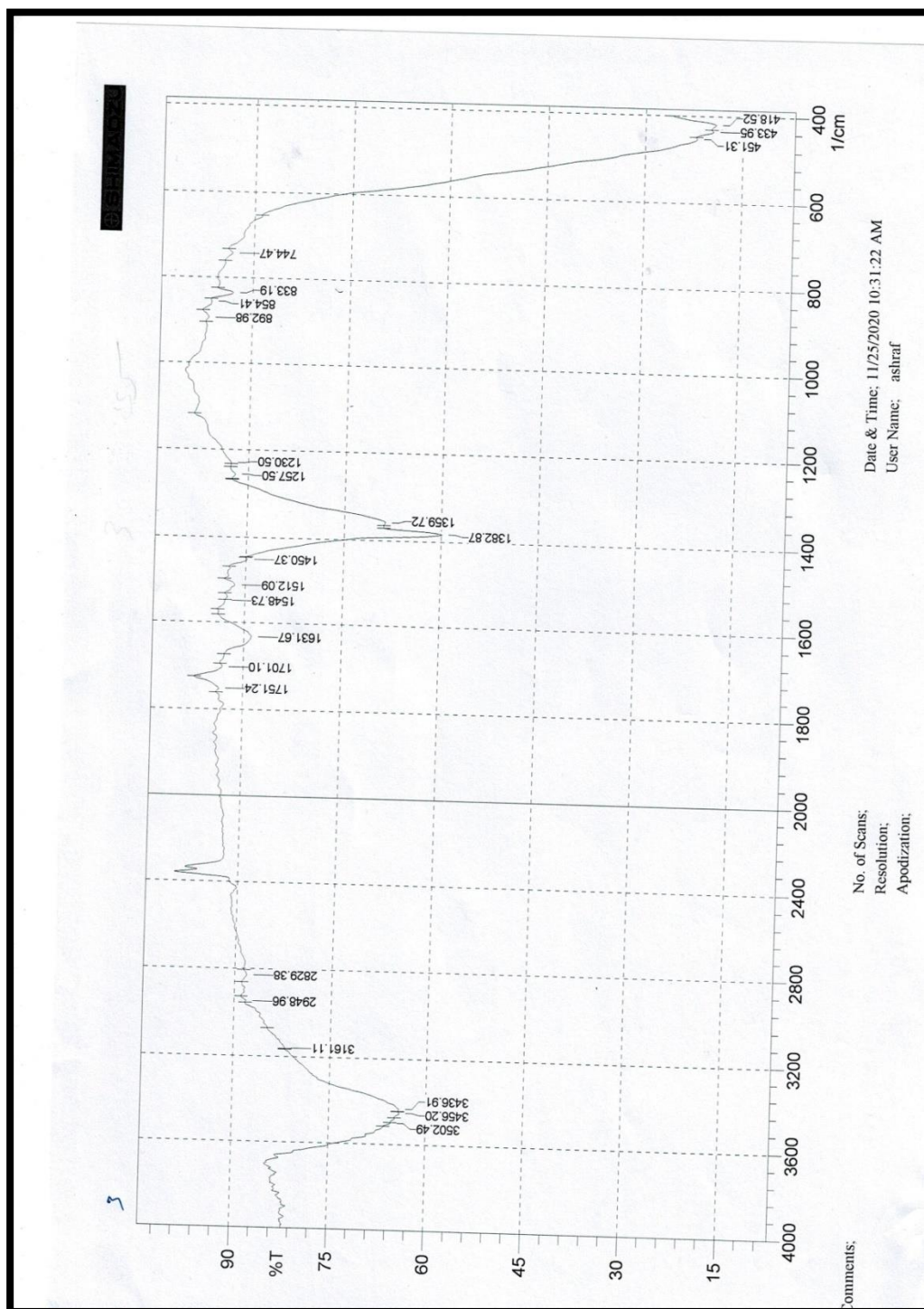
The average particle sizes was 50 nm

**Figure(3)**

### 3.4.FTIR spectra

The FTIR spectra of untreated and treated glass mat was investigated in the spectral range of 600–4000  $\text{cm}^{-1}$ . NiO's FTIR chart has been organized. As can be seen in Figure (4) the peak, which belonged to the FTIR performance, was discovered to be in the 4000e400  $\text{cm}^{-1}$  region. Furthermore, the peaks have been discovered at 451, 1382, and 3456  $\text{cm}^{-1}$ <sup>[13]</sup>. The stretching vibration of Ni-O has been assigned to the observed wide peak In the 450-855  $\text{cm}^{-1}$  region. However, based on the width of observed peaks, we have assumed that the crystals of NiO were in nanoparticles. The wide absorption band at 3456  $\text{cm}^{-1}$  was thought to be related to stretching vibrations of O—H<sup>[14]</sup>, while a weedy peak about 1382  $\text{cm}^{-1}$  was thought to be related to H-O-H bending, which is normally the product of water adsorption in air. Furthermore, the two bands at about 3456 and 1382  $\text{cm}^{-1}$  may have been caused by existing water molecules (absorbed by the NiONPs or NaOH).

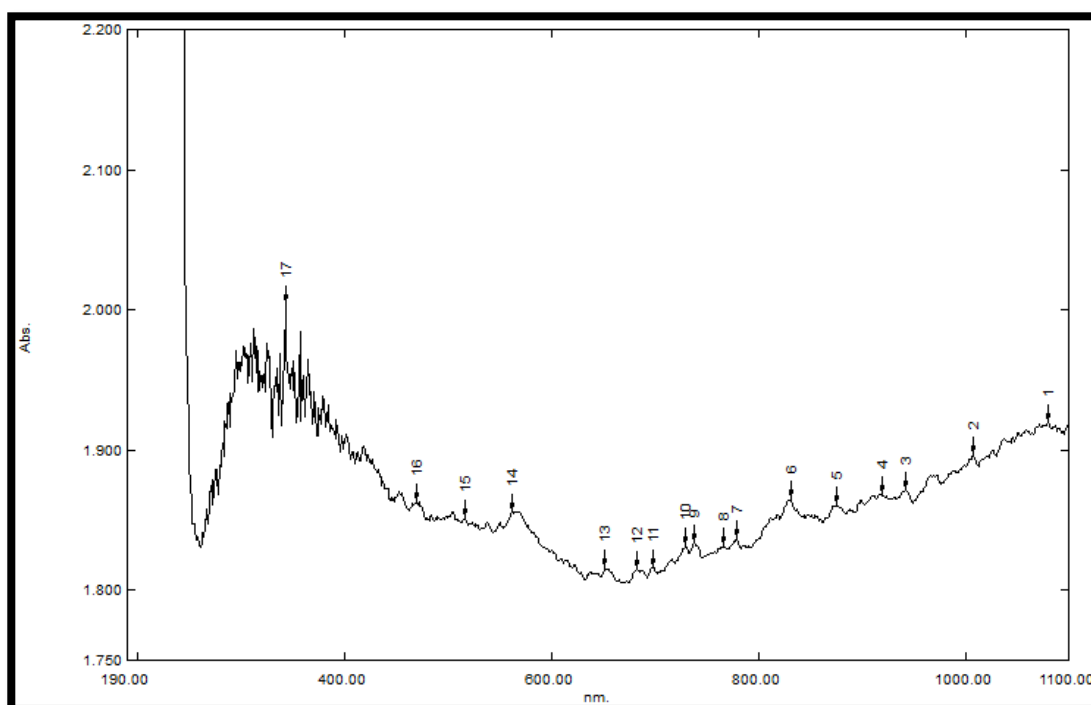




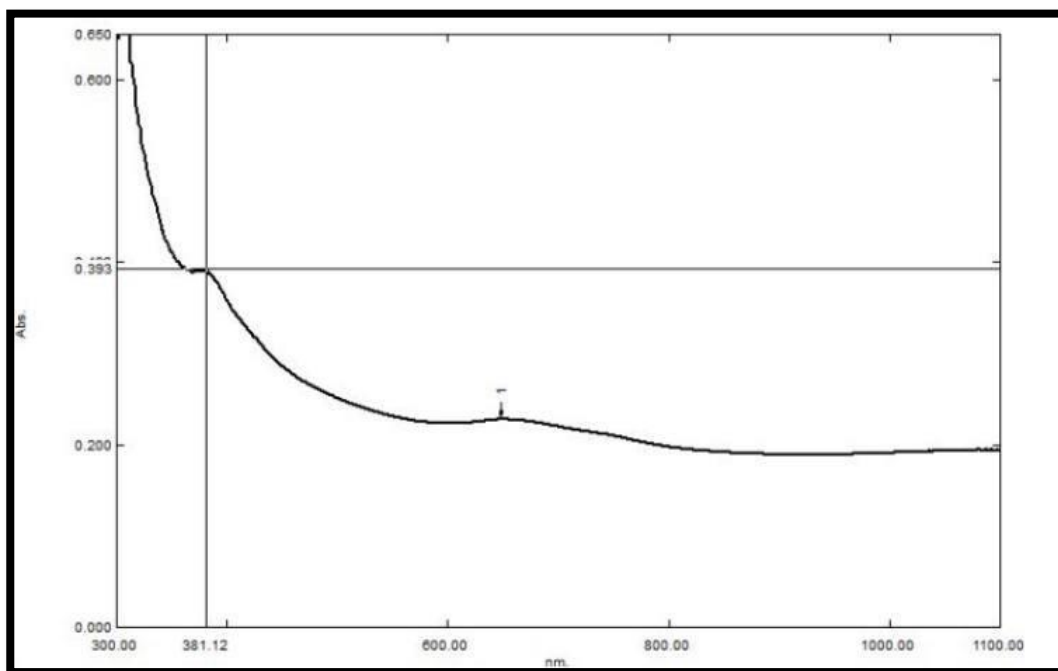
### **Figure(4) :The Analysis of (FT-IR) of NiO nanoparticles by sol-gel**

#### **3.5.UV-VIS spectra**

Ultraviolet absorption is a process in which the outer electrons of atoms or molecules absorb radiant energy and undergo transitions to high energy levels. Figure(5) shows the UV-Vis absorption spectra of the synthesized NiO by sol-gel, . The observed spectrum revealed an adsorption edge at 300–400 nm, suggesting a bandgap of 3–4 eV for the synthesized NiO. We plotted  $(h\nu)^2$  as a function of  $h\nu$  to determine the bandgap of NiO nanoplates, where,  $h$ , and  $\nu$  denote the absorption coefficient, Planck constant, and frequency, respectively. The optical bandgap of NiO nanoplates was calculated as 3.45 eV by extrapolating the linear portion of the curve. This figure was significantly lower than the previously recorded figure of 3.7 eV<sup>[13]</sup>







**Figure(5) shows the UV-Vis absorption spectra of the synthesized NiO by sol-gel**

### Conclusion

NiO Sol-Gel nanotechnology was successfully used at 75 °C and pH 12 in NaOH. The average crystal size of NiO nanoparticles was determined by X-ray diffraction tests to be 40 nm, 61 nm, 39 nm and the SEM image gave sizes ranging (26.80nm\_37.96nm). Matches the sizes between the AFM device nm, and 45 nm In the ultraviolet and visible ranges, the absorption spectra of NiO NPs display a blue color The peak is at 381 nm.

### References

1. Sonia, M.M.L., S. Blessi, and S. Pauline, *Role of lanthanum substitution on the structural and magnetic properties of nanocrystalline nickel ferrites*. International Journal of Advance Research in Science and Engineering, IJARSE, 2014. **3**(7): p. 360-367.
2. Kumar, A., et al., *Sol-gel derived nanomaterials and it's applications: a review*. Research Journal of Chemical Sciences ISSN, 2015. **2231**: p. 606X.
3. Almashhadani, H. and K. Alsaadie, *Corrosion Protection of Carbon Steel in seawater by alumina nanoparticles with poly (acrylic acid) as charging agent*. Moroccan Journal of Chemistry, 2018. **6**(3): p. 6-3 (2018) 455-465.
4. AlMashhadani, H.A. and K.A. saleh, *Electrochemical Deposition of Hydroxyapatite Co-Substituted By Sr/Mg Coating on Ti-6Al-4V ELI Dental Alloy Post-MAO as Anti-Corrosion*. Iraqi Journal of Science, 2020. **61**(11): p. 2751-2761.

5. Srinivas, B., et al., *Review on present and advance materials for solar cells*. International Journal of Engineering Research-Online, 2015. **3**: p. 178-182.
6. Bagher, A.M., M.M.A. Vahid, and M. Mohsen, *Types of solar cells and application*. American Journal of optics and Photonics, 2015. **3**(5): p. 94-113.
7. AlMashhadani, H.A. and K.A. saleh, *Electro-polymerization of poly Eugenol on Ti and Ti alloy dental implant treatment by micro arc oxidation using as Anti-corrosion and Anti-microbial*. Research Journal of Pharmacy and Technology, 2020. **13**(10): p. 4687-4696.
8. Hayfaa, A.A., A.S.A. Khulood, and H.A.Y. AlMashhadani. *Study the Effect of Cyperus Rotundus Extracted as Mouthwash on the Corrosion of Dental Amalgam*. in *IOP Conf. Series: Materials Science and Engineering*. 2019.
9. Mironova-Ulmane, N., et al. *Structural and magnetic properties of nickel oxide nanopowders*. in *Solid State Phenomena*. 2011. Trans Tech Publ.
10. Al-Hajry, A., et al., *Low-temperature growth and properties of flower-shaped  $\beta$ -Ni (OH) 2 and NiO structures composed of thin nanosheets networks*. Superlattices and Microstructures, 2008. **44**(2): p. 216-222.
11. Javed, H.M.A., et al., *Perspective of nanomaterials in the performance of solar cells*, in *Solar cells*. 2020, Springer. p. 25-54.
12. Pooyandeh, S., et al., *Synthesizing and deposition of nickel oxide nanoparticles on glass mat using sol-gel method (morphological and magnetic properties)*. The Journal of The Textile Institute, 2021. **112**(6): p. 887-895.
13. Ghazal, S., et al., *Sol-gel biosynthesis of nickel oxide nanoparticles using Cydonia oblonga extract and evaluation of their cytotoxicity and photocatalytic activities*. Journal of Molecular Structure, 2020. **1217**: p. 128378.
14. Sabouri, Z., et al., *Eco-friendly biosynthesis of nickel oxide nanoparticles mediated by okra plant extract and investigation of their photocatalytic, magnetic, cytotoxicity, and antibacterial properties*. Journal of Cluster Science, 2019. **30**(6): p. 1425-1434.